A Novel *NM*-Polynomial Approach to *QSPR* Analysis of Anti-Diabetic Drugs Using Neighborhood Degree-Based Topological indices

Masoud Ghods

Department of Applied Mathematics, Semnan University, Semnan 35131-19111, Iran
mghods@semnan.ac.ir

Ali Asghar Talebi*

Department of Mathematics, University of Mazandaran, Babolsar, 4741613534, Iran
a.talebi@umz.ac.ir (corresponding author)

Muntaha Khudhair Abbas

Middle Technical University Bghdad - Technical college of management baghdad, Iraq
muntaha2018@mtu.edu.iq

Jaber Ramezani Tousi

Department of Mathematics, University of Mazandaran, Babolsar, 4741613534, Iran
j.ramzani@umail.umz.ac.ir

Arezo Esmaeili

Department of Applied Mathematics, Semnan University, Semnan 35131-19111, Iran
Arezo.esmaeili@semnan.ac.ir

Negar Kheirkhahan
Department of Applied Mathematics, Semnan University, Semnan 35131-19111, Iran
Negar.kheirkhahan@semnan.ac.ir

ABSTRACT

Diabetes mellitus, a complex metabolic disorder, necessitates the continuous development of effective therapeutics. In this article, we employ a Quantitative Structure-Property Relationship (*QSPR*) paradigm to analyze ten prominent antidiabetic drugs. Using chemical graph theory, the molecular graphs of these drugs were constructed, and an advanced computational framework based on the *NM*-polynomial was utilized to simultaneously derive thirteen neighborhood degree sum-based topological indices (*TI*). These indices, including the Neighborhood Zagreb indices, Neighborhood Harmonic index, and Neighborhood Inverse Sum index, served as numerical descriptors to model eight crucial physicochemical properties: Boiling Point (BP), Enthalpy of Vaporization (*EV*), Flash Point (*FP*), Molar Refractivity (*MR*), Polar Surface Area (*PSA*), Polarizability (*PO*), Molar Volume (*MV*), and Refractive Index (*IR*). Linear regression models revealed strong and statistically significant correlations ($p < 0.05$) between these topological indices and the drug properties. Specifically, the Neighborhood Modified Second Zagreb index (NmM_2) showed the highest correlation with *BP* and *MV* ($r = 0.920$ and $r = 0.945$, respectively), while the Neighborhood Sum Connectivity index (*NSCI*) was a superior predictor for *MR* and *PO* ($r = 0.969$ for both). These results validate the predictive power of the *NM*-polynomial approach and underscore its efficacy as a reliable computational tool for the design and optimization of antidiabetic drugs with desirable physicochemical profiles. The findings of this article can pave the way for developing the next generation of diabetes therapeutics.

KEYWORDS: *NM*-polynomial, *QSPR*, Topological indices, Antidiabetic Drugs, Physicochemical Properties, Linear Regression.

1. Introduction

Diabetes mellitus, a chronic metabolic disorder characterized by hyperglycemia, has emerged as a global health challenge of epidemic proportions [1]. Its management predominantly relies on pharmacological interventions to regulate blood glucose levels and prevent long-term complications [2]. The efficacy and physicochemical properties of these antidiabetic drugs are intrinsically linked to their molecular structure. Consequently, predicting these properties computationally, prior to costly and time-consuming synthetic procedures, is a paramount objective in modern pharmaceutical research and development.

Quantitative Structure-Property Relationship (*QSPR*) modeling serves as a powerful in-silico tool in this endeavor, establishing mathematical correlations between the structural features of compounds and their biological or physicochemical activities [3, 4, 18]. Within the *QSPR* paradigm, topological indices (*TIs*)—numerical descriptors derived from the molecular graph—have proven invaluable [21, 22]. These indices, foundational to chemical graph theory, condense complex structural information into single numerical values, providing profound insights into properties such as boiling point, molar refractivity, and bioavailability without the need for experimental assays [5, 6]. Traditional degree-based TIs have been extensively studied [7]; however, there is a growing interest in more sophisticated descriptors that capture a richer topological landscape.

Recently, neighborhood degree sum-based topological indices have garnered significant attention for their enhanced discriminatory power in capturing the influence of a vertex's immediate chemical environment [8, 9]. These indices offer a more nuanced representation of molecular connectivity compared to classical degree-based indices. The *NM*-polynomial, a novel generating function, has been introduced as an efficient and versatile tool for computing a wide spectrum of these neighborhood degree sum-based *TIs* simultaneously [10, 11]. This approach streamlines the calculation process and facilitates a comprehensive topological analysis of complex molecular structures.

While several studies have applied *TIs* to various chemical compounds [12, 13, 19, 20], a focused and systematic *QSPR* analysis of a curated set of prominent antidiabetic drugs using this advanced *NM*-polynomial framework remains largely unexplored. This research gap presents a significant opportunity to leverage cutting-edge mathematical chemistry for drug design optimization. Recent work has demonstrated the effectiveness of similar approaches for other drug classes, indicating the potential of this method [14, 15].

In this article, we bridge this gap by conducting a rigorous *QSPR* analysis of ten fundamental antidiabetic medications: Gliclazide, Sitagliptin, Vildagliptin, Nateglinide, Tolazamide, Metformin, Miglitol, Empagliflozin, Tolbutamide, and Chlorpropamide. Our primary objectives are:

1. To construct the molecular graphs of these drugs and compute their respective *NM*-polynomials.

2. To derive a suite of thirteen key neighborhood degree sum-based topological indices (e.g., Neighborhood Zagreb indices, Neighborhood Harmonic index, Neighborhood Inverse Sum index) from these polynomials [10, 16, 17].
3. To establish robust linear *QSPR* models that correlate these topological descriptors with critical physicochemical properties, including Boiling Point (*BP*), Enthalpy of Vaporization (*EV*), Flash Point (*FP*), Molar Refractivity (*MR*), Polar Surface Area (*PSA*), Polarizability (*PO*), Molar Volume (*MV*), and Refractive index (*IR*).

The findings of this investigation demonstrate a remarkably strong correlation between the proposed indices and the target properties, validating the utility of the *NM*-polynomial approach. We anticipate that the developed models will serve as reliable predictive tools, accelerating the design and optimization of next-generation antidiabetic agents with improved efficacy and tailored physicochemical profiles.

The remainder of this article is structured as follows: Section 2 details the materials and methods, including the computation of *NM*-polynomials and topological indices. Section 3 presents the results of the *QSPR* modeling and a detailed discussion of the correlations. Finally, the article concludes with a summary of the key findings and their potential implications in Section 4.

2 MATERIAL AND METHOD

In the molecular configurations of medications, atoms are modeled as vertices, while the bonds that connect these atoms are represented as edges. The graph $H= (V, W)$ is defined as an unweighted, finite, and cohesive graph, where V and W denote the collections of nodes and edges, correspondingly, within the chemical graph. The degree of a node s in graph H is defined as the sum of the degrees of the adjacent vertices with it, represented as $n\delta(s)$. In the context of chemistry, the valence of an atom is closely related to its connectivity within the molecular structure [11-13]. The formula for calculating the *TIs* is given in Table (1). Due to its extensive applicability, the derivation of the formulas for neighborhood degree sum-based *TI* is given in various articles. For further reading, refer to references [14-20].

Table 1. Exploration of *TIs* and their formulation via *NM*-polynomial.

TI	***Formula H(Π(r), Π(s))***	***ħ (p, q) = NM (H; p, q)***
Neighborhood First Zagreb: NM_1	$\sum_{rs\in W(H)} (\eta(r)+\eta(s))$	$(\Psi_p+\Psi_q)(\hbar(p,q))\big\vert_{p=q=1}$
Neighborhood Second Zagreb: NM_2	$\sum_{rs\in W(H)} \eta(r)\eta(s)$	$(\Psi_p\Psi_q)(\hbar(p,q))\big\vert_{p=q=1}$
Neighborhood Redefined Third Zagreb: $NRezM_3$	$\sum_{rs\in W(H)} \eta(r)\eta(s)(\eta(r)+\eta(s))$	$(\Psi_p\Psi_q)(\Psi_p+\Psi_q)(\hbar(p,q))\big\vert_{p=q=1}$
Neighborhood Modified Second Zagreb: NmM_2	$\sum_{rs\in W(H)} \frac{1}{\eta(r)\eta(s)}$	$S_pS_q(\hbar(p,q))\big\vert_{p=q=1}$
Neighborhood Forgotten Topological: *NF*	$\sum_{rs\in W(H)} (\eta^2(r)+\eta^2(s))$	$(\Psi_p^2+\Psi_q^2)(\hbar(p,q))\big\vert_{p=q=1}$

Neighborhood Symmetric Division: *NSDD*	$\sum_{rs\in W(H)} \frac{(\eta^2(r)+\eta^2(s))}{\eta(r)\eta(s)}$	$\left(\Psi_p S_q + S_p \Psi_q\right)\left(\hbar(p,q)\right)\big\vert_{p=q=1}$
Neighborhood Harmonic Index: *NH*	$\sum_{rs\in W(H)} \frac{2}{\eta(r)+\eta(s)}$	$2S_p J\left(\hbar(p,q)\right)\big\vert_{p=1}$
Neighborhood Inverse Sum Index: *NISI*	$\sum_{rs\in W(H)} \frac{\eta(r)\eta(s)}{\eta(r)+\eta(s)}$	$S_p J\Psi_p\Psi_q\left(\hbar(p,q)\right)\big\vert_{p=1}$
Neighborhood Augmented Zagreb Index: *NAZI*	$\sum_{rs\in W(H)} \left(\frac{\eta(r)\eta(s)}{\eta(r)+\eta(s)-2}\right)^3$	$S_p^3 Q_{-2} J\Psi_p^3\Psi_q^3\left(\hbar(p,q)\right)\big\vert_{p=1}$
Neighborhood Sum Connectivity Index: *NSCI*	$\sum_{rs\in W(H)} \frac{1}{\sqrt{\eta(r)+\eta(s)}}$	$S_p^{\frac{1}{2}} J\left(\hbar(p,q)\right)\big\vert_{p=1}$
Neighborhood Inverse Randić Index: *NIR*	$\sum_{rs\in W(H)} \frac{1}{\sqrt{\eta(r)\eta(s)}}$	$S_p^{\frac{1}{2}} S_q^{\frac{1}{2}}\left(\hbar(p,q)\right)\big\vert_{p=q=1}$
Neighborhood Ordinary Geometric Arithmetic Index: *OGA*	$\sum_{rs\in W(H)} \frac{2\sqrt{\eta(r)\eta(s)}}{(\eta(r)+\eta(s))}$	$2S_p J\Psi_p^{\frac{1}{2}}\Psi_q^{\frac{1}{2}}\left(\hbar(p,q)\right)\big\vert_{p=1}$
Neighborhood Atomic Bond Connectivity Index: *NABC*	$\sum_{rs\in W(H)} \sqrt{\frac{\eta(r)+\eta(s)-2}{\eta(r)\eta(s)}}$	$S_p^{\frac{1}{2}} Q_{-2} J\left(\Psi_p^{\frac{1}{2}}+\Psi_q^{\frac{1}{2}}\right)\left(\hbar(p,q)\right)\big\vert_{p=1}$

$\Psi_p = p\left(\frac{\partial\hbar(p,q)}{\partial p}\right)$, $\Psi_q = q\left(\frac{\partial\hbar(p,q)}{\partial q}\right)$, $S_p = \int_0^p \frac{\hbar(t,q)}{t}dt$, $S_q = \int_0^q \frac{\hbar(p,t)}{t}dt$, $J\hbar(p,q) = \hbar(p,p)$, $Q_k\hbar(p) = p^k\hbar(p)$.

For neighborhood degree sum-based *TI*: $\eta(r) = n\delta(r), \eta(s) = n\delta(s), \hbar(p,q) = NM(H;p,q)$.

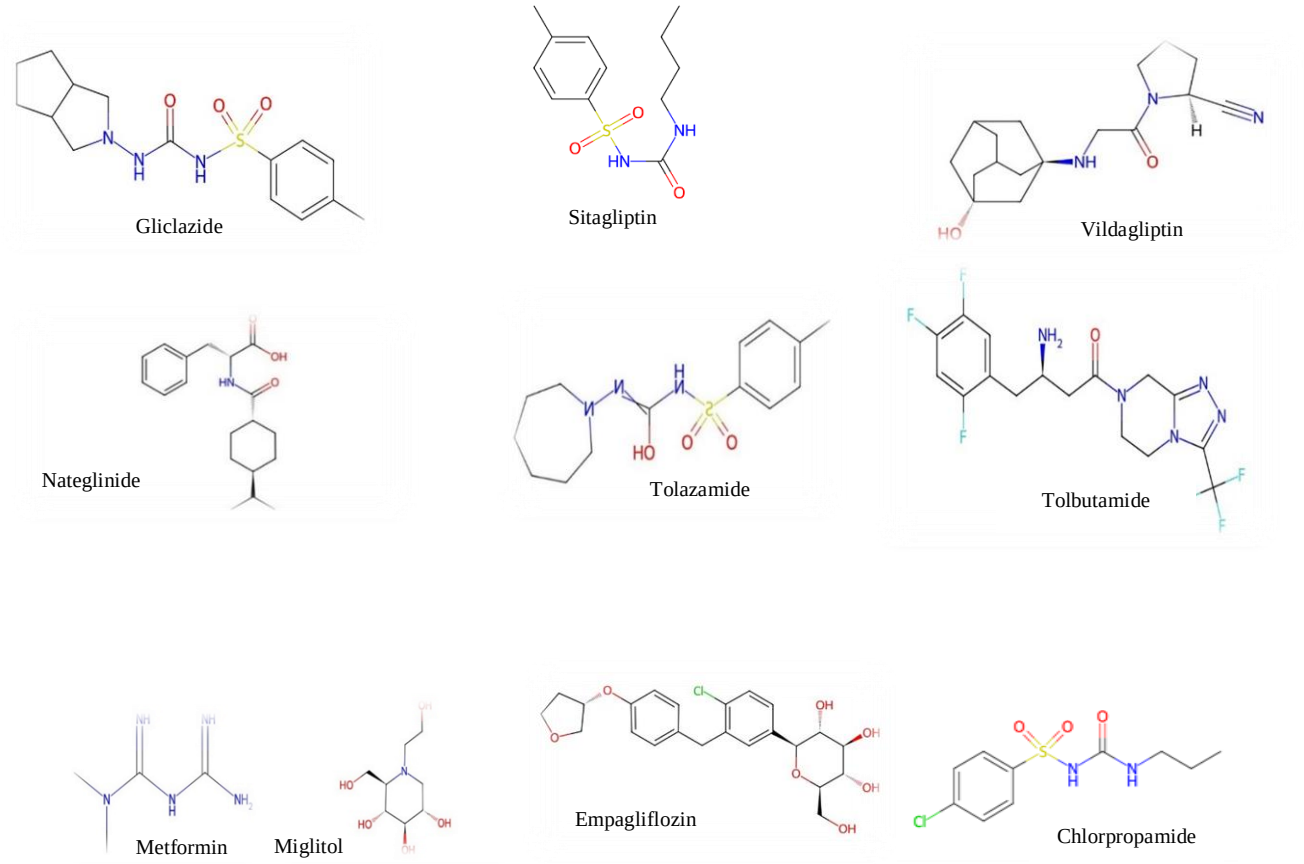

Fig. 1. Molecular structure of Gliclazide, Sitagliptin, Vildagliptin, Nateglinide, Tolazamide, Metformin, Miglitol, Empagliflozin, Tolbutamide, Chlorpropamide.

Theorem 1. Assuming that *GL* represents Gliclazide, the following relationship is established:

$$NM\left(GL;p,q\right)=2p^3q^5+2p^4q^5+2p^4q^7+4p^5q^5+p^5q^6+3p^5q^7+2p^5q^8+3p^6q^6+2p^6q^7+2p^7q^7+p^7q^8.$$

Proof: Figure 2 illustrates the Gliclazide graph. Observing that, we can conclude that $\left|V(GL)\right|=22$ and $\left|W(GL)\right|=24$.

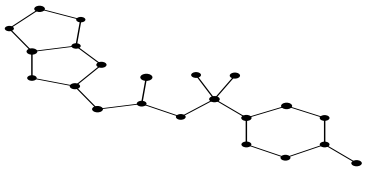

Fig. 2. Molecular graph of Gliclazide (GL).

In the framework of structural examination, the edge collection of Gliclazide (GL) can be categorized into eleven distinct groups, as delineated below, according to the degrees of the vertices:

$$W_{35}^{*}=\left\{rs\in W(GL)\middle|\, n\delta(r)=3,\ n\delta(s)=5\right\},\ W_{45}^{*}=\left\{rs\in W(GL)\middle|\, n\delta(r)=4,\ n\delta(s)=5\right\},$$
$$W_{47}^{*}=\left\{rs\in W(GL)\middle|\, n\delta(r)=4,\ n\delta(s)=7\right\},\ W_{55}^{*}=\left\{rs\in W(GL)\middle|\, n\delta(r)=5,\ n\delta(s)=5\right\},$$
$$W_{56}^{*}=\left\{rs\in W(GL)\middle|\, n\delta(r)=5,\ n\delta(s)=6\right\},\ W_{57}^{*}=\left\{rs\in W(GL)\middle|\, n\delta(r)=5,\ n\delta(s)=7\right\},$$
$$W_{58}^{*}=\left\{rs\in W(GL)\middle|\, n\delta(r)=5,\ n\delta(s)=8\right\},\ W_{66}^{*}=\left\{rs\in W(GL)\middle|\, n\delta(r)=6,\ n\delta(s)=6\right\},$$
$$W_{67}^{*}=\left\{rs\in W(GL)\middle|\, n\delta(r)=6,\ n\delta(s)=7\right\},\ W_{77}^{*}=\left\{rs\in W(GL)\middle|\, n\delta(r)=7,\ n\delta(s)=7\right\},$$
$$W_{78}^{*}=\left\{rs\in W(GL)\middle|\, n\delta(r)=7,\ n\delta(s)=8\right\}.$$
$$\left|W_{35}^{*}\right|=2,\ \left|W_{45}^{*}\right|=2,\ \left|W_{47}^{*}\right|=2,\ \left|W_{55}^{*}\right|=4,\ \left|W_{56}^{*}\right|=1,\ \left|W_{57}^{*}\right|=3,\ \left|W_{58}^{*}\right|=2,\ \left|W_{66}^{*}\right|=3,\ \left|W_{67}^{*}\right|=2,$$
$$\left|W_{77}^{*}\right|=2,\ \left|W_{78}^{*}\right|=1.$$

By a designation of *NM*-polynomial

$$NM\left(H;p,q\right)=\sum_{\alpha\le\beta}m_{\alpha\beta}^{*}(H)p^{\alpha}q^{\beta}.$$

$$NM\left(GL;p,q\right)=\sum_{3\le5}m_{35}^{*}p^3q^5+\sum_{4\le5}m_{45}^{*}p^4q^5+\sum_{4\le7}m_{47}^{*}p^4q^7+\sum_{5\le5}m_{55}^{*}p^5q^5+\sum_{5\le6}m_{56}^{*}p^5q^6+\sum_{5\le7}m_{57}^{*}p^5q^7+\sum_{5\le8}m_{58}^{*}p^5q^8$$
$$+\sum_{6\le6}m_{66}^{*}p^6q^6+\sum_{6\le7}m_{67}^{*}p^6q^7+\sum_{7\le7}m_{77}^{*}p^7q^7+\sum_{7\le8}m_{78}^{*}p^7q^8.$$
$$NM\left(GL;p,q\right)=2q^3q^5+2p^4q^5+2p^4q^7+4p^5q^5+p^5q^6+3p^5q^7+2p^5q^8+3p^6q^6+2p^6q^7+2p^7q^7+p^7q^8.$$

The spatial depiction of *NM*-polynomials for Gliclazide is depicted in Fig. 3 below.

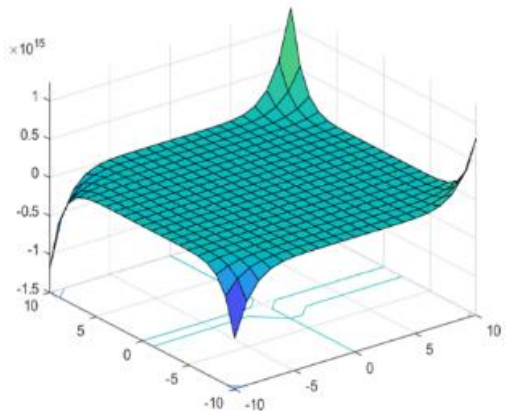

Fig. 3: Scheme of *NM*-Polynomial for Gliclazide.

In the following proposition, we derive several *TIs* of Gliclazide.

Proposition 1 Let GL represent the graph of Gliclazide. The following relationships are defined:

1. $NM_1(GL) = 274.$
2. $NM_2(GL) = 787.$
3. $NmM_2(GL) = 0.82.$
4. $ND_3(GL) = 9446.$
5. $NF(GL) = 1636.$
6. $ND_5(GL) = 50.17.$
7. $NIR(GL) = 4.32.$
8. $NH(GL) = 4.32.$
9. $NISI(GL) = 67.1.$
10. $S(GL) = 942.75.$
11. $NSCI(GL) = 7.09.$
12. $NOGA(GL) = 9.94.$
13. $NABC(GL) = 37.32.$

Proof:

$$NM(GL;p,q)=\hbar(p,q)=2p^3q^5+2p^4q^5+2p^4q^7+4p^5q^5+p^5q^6+3p^5q^7+2p^5q^8+3p^6q^6+2p^6q^7+2p^7q^7+p^7q^8.$$

$$\Psi_p\hbar(p,q)=6p^3q^5+8p^4q^5+8p^4q^7+20p^5q^5+5p^5q^6+15p^5q^7+10p^5q^8+18p^6q^6+12p^6q^7+14p^7q^7+7p^7q^8.$$

$$\Psi_q\hbar(p,q)=10p^3q^5+10p^4q^5+14p^4q^7+20p^5q^5+6p^5q^6+21p^5q^7+16p^5q^8+18p^6q^6+14p^6q^7+14p^7q^7+8p^7q^8.$$

$$(\Psi_p+\Psi_q)(\hbar(p,q))=16p^3q^5+18p^4q^5+22p^4q^7+40p^5q^5+11p^5q^6+36p^5q^7+26p^5q^8+36p^6q^6+26p^6q^7+28p^7q^7+15p^7q^8.$$

$$\Psi_p\Psi_q(\hbar(p,q))=30p^3q^5+40p^4q^5+56p^4q^7+100p^5q^5+30p^5q^6+105p^5q^7+80p^5q^8+108p^6q^6+84p^6q^7+98p^7q^7+56p^7q^8.$$

$$\Psi_p^k\Psi_q^k(\hbar(p,q))=3^k5^k2p^3q^5+4^k5^k2p^4q^5+4^k7^k2p^4q^7+5^k5^k4p^5q^5+5^k6^kp^5q^6+5^k7^k3p^5q^7+5^k8^k2p^5q^8+6^k6^k3p^6q^6+6^k7^k2p^6q^7+7^k7^k2p^7q^7+7^k8^kp^7q^8.$$

$$S_pS_q(\hbar(p,q))=\frac{2}{15}p^3q^5+\frac{2}{20}p^4q^5+\frac{2}{28}p^4q^7+\frac{4}{25}p^5q^5+\frac{1}{30}p^5q^6+\frac{3}{35}p^5q^7+\frac{2}{40}p^5q^8+\frac{3}{36}p^6q^6+\frac{2}{49}p^7q^7+\frac{1}{21}p^6q^7+\frac{1}{56}p^7q^8.$$

$$S_p^kS_q^k(\hbar(p,q))=\frac{2}{3^k5^k}p^3q^5+\frac{2}{4^k5^k}p^4q^5+\frac{2}{4^k7^k}p^4q^7+\frac{4}{5^k5^k}p^5q^5+\frac{1}{5^k6^k}p^5q^6+\frac{3}{5^k7^k}p^5q^7+\frac{2}{5^k8^k}p^5q^8+\frac{3}{6^k6^k}p^6q^6+\frac{2}{6^k7^k}p^6q^7+\frac{2}{7^k7^k}p^7q^7+\frac{1}{7^k8^k}p^7q^8.$$

$$(\Psi_p^2+\Psi_q^2)(\hbar(p,q))=68p^3q^5+82p^4q^5+130p^4q^7+200p^5q^5+61p^5q^6+222p^5q^7+178p^5q^8+216p^6q^6+170p^6q^7+196p^7q^7+113p^7q^8.$$

$$\Psi_p\Psi_q(\Psi_p+\Psi_q)(\hbar(p,q))=240p^3q^5+360p^4q^5+616p^4q^7+1000p^5q^5+330p^5q^6+1260p^5q^7+1040p^5q^8+1296p^6q^6+1092p^6q^7+1372p^7q^7+840p^7q^8.$$

$$S_pJ(\hbar(p,q))=\frac{1}{4}p^8+\frac{2}{9}p^9+\frac{3}{11}p^{11}+\frac{2}{5}p^{10}+\frac{1}{2}p^{12}+\frac{4}{13}p^{13}+\frac{1}{7}p^{14}+\frac{1}{15}p^{15}.$$

$$S_pJ\Psi_p\Psi_q(\hbar(p,q))=\frac{15}{4}p^8+\frac{40}{9}p^9+\frac{86}{11}p^{11}+10p^{10}+\frac{213}{12}p^{12}+\frac{164}{13}p^{13}+\frac{98}{14}p^{14}+\frac{56}{15}p^{15}.$$

$$S_p^3Q_{-2}J\Psi_p^3\Psi_q^3(\hbar(p,q))=\frac{6750}{216}p^6+\frac{16000}{343}p^7+\frac{70904}{729}p^9+\frac{62500}{512}p^8+\frac{268593}{1000}p^{10}+\frac{276176}{1331}p^{11}+\frac{235298}{1728}p^{12}+\frac{175616}{2197}p^{13}.$$

$$S_p^{\frac{1}{2}}J(\hbar(p,q))=\frac{2}{\sqrt{8}}p^8+\frac{2}{3}p^9+\frac{3}{\sqrt{11}}p^{11}+\frac{4}{\sqrt{10}}p^{10}+\frac{6}{\sqrt{12}}p^{12}+\frac{4}{\sqrt{13}}p^{13}+\frac{2}{\sqrt{14}}p^{14}+\frac{1}{\sqrt{15}}p^{15}.$$

$$S_p^{\frac{1}{2}}S_q^{\frac{1}{2}}(\hbar(p,q))=\frac{2\sqrt{15}}{15}p^3q^5+\frac{\sqrt{20}}{10}p^4q^5+\frac{\sqrt{28}}{14}p^4q^7+\frac{4}{5}p^5q^5+\frac{\sqrt{30}}{30}p^5q^6+\frac{3\sqrt{35}}{35}p^5q^7+\frac{\sqrt{10}}{10}p^5q^8+\frac{3}{6}p^6q^6+\frac{2}{\sqrt{42}}p^6q^7+\frac{2}{7}p^7q^7+\frac{1}{\sqrt{56}}p^7q^8.$$

$$S_p^{\frac{1}{2}}Q_{-2}J\left(\Psi_p^{\frac{1}{2}}+\Psi_q^{\frac{1}{2}}\right)(\hbar(p,q))=3.24p^6+3.20p^7+3.09p^9+6.32p^8+1.55p^9+4.62p^{10}+3.05p^{11}+4.63p^{10}+3.06p^{11}+3.05p^{12}+1.51p^{13}.$$

Now we have:

1. $NM_1(GL) = \left(\Psi_p + \Psi_q\right)\left(\hbar(p,q)\right)\big|_{p=q=1} = 274.$
2. $NM_2(GL) = \Psi_p \Psi_q \hbar(p,q)\big|_{p=q=1} = 787.$
3. $NmM_2(GL) = S_p S_q \hbar(p,q)\big|_{p=q=1} = 0.82.$
4. $ND_3(GL) = \Psi_p \Psi_q \left(\Psi_p + \Psi_q\right)\hbar(p,q)\big|_{p=q=1} = 9446.$
5. $NF(GL) = \left(\Psi_p^2 + \Psi_q^2\right)\hbar(p,q)\big|_{p=q=1} = 1636.$
6. $ND_S(GL) = \left(S_q \Psi_p + S_p \Psi_q\right)\hbar(p,q)\big|_{p=q=1} = 50.17.$
7. $NIR(GL) = S_p^{\frac{1}{2}} S_q^{\frac{1}{2}}\left(\hbar(p,q)\right)\big|_{p=q=1} = 4.32.$
8. $NH(GL) = 2S_p J\left(\hbar(p,q)\right)\big|_{p=q=1} = 4.32.$
9. $NISI(GL) = S_p J \Psi_p \Psi_q \left(\hbar(p,q)\right)\big|_{p=q=1} = 67.1.$
10. $S(GL) = S_p^3 Q_{-2} J \Psi_p^3 \Psi_q^3 \left(\hbar(p,q)\right)\big|_{p=q=1} = 942.75.$
11. $NSCI(GL) = S_p^{\frac{1}{2}} J\left(\hbar(p,q)\right)\big|_{p=q=1} = 7.09.$
12. $NOGA(GL) = 2S_p J \Psi_p^{\frac{1}{2}} \Psi_q^{\frac{1}{2}}\left(\hbar(p,q)\right)\big|_{p=q=1} = 9.94.$
13. $NABC(GL) = S_p^{\frac{1}{2}} Q_{-2} J\left(\Psi_p^{\frac{1}{2}} + \Psi_q^{\frac{1}{2}}\right)\left(\hbar(p,q)\right)\big|_{p=q=1} = 37.32.$

Theorem 2. Assuming that *SI* represents Sitagliptin, the following relationship is established:

$$NM(SI;p,q) = p^3q^5 + 4p^3q^6 + 3p^4q^6 + 2p^5q^5 + 2p^5q^6 + 2p^5q^7 + p^5q^8 + p^5q^9 + 5p^6q^6 + 6p^6q^7 + p^6q^9 + p^7q^8 + p^8q^9.$$

Proof: Figure 4 illustrates the Sitagliptin graph. Observing that, we can conclude that $|V(SI)| = 28$ and $|W(SI)| = 30$.

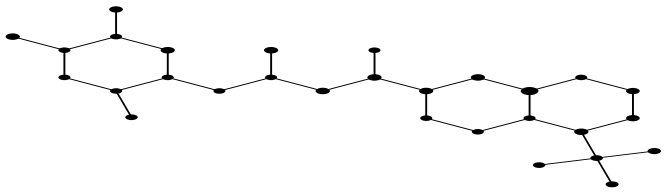

Fig. 4: Molecular graph of Sitagliptin (*SI*).

In the framework of structural examination, the edge collection of Sitagliptin (SI) can be categorized into twelve distinct groups, as delineated below, according to the degrees of the vertices:

$$W_{35}^{*}=\{rs\in W(SI)|n\delta(r)=3,n\delta(s)=5\},W_{36}^{*}=\{rs\in W(SI)|n\delta(r)=3,n\delta(s)=6\},$$
$$W_{46}^{*}=\{rs\in W(SI)|n\delta(r)=4,n\delta(s)=6\},W_{55}^{*}=\{rs\in W(SI)|n\delta(r)=5,n\delta(s)=5\},$$
$$W_{57}^{*}=\{rs\in W(SI)|n\delta(r)=5,n\delta(s)=7\},W_{58}^{*}=\{rs\in W(SI)|n\delta(r)=5,n\delta(s)=8\},$$
$$W_{59}^{*}=\{rs\in W(SI)|n\delta(r)=5,n\delta(s)=9\},W_{66}^{*}=\{rs\in W(SI)|n\delta(r)=6,n\delta(s)=6\},$$
$$W_{67}^{*}=\{rs\in W(SI)|n\delta(r)=6,n\delta(s)=7\},W_{69}^{*}=\{rs\in W(SI)|n\delta(r)=6,n\delta(s)=9\},$$
$$W_{78}^{*}=\{rs\in W(SI)|n\delta(r)=7,n\delta(s)=8\},W_{89}^{*}=\{rs\in W(SI)|n\delta(r)=8,n\delta(s)=9\},$$
$$|W_{35}^{*}|=1,|W_{36}^{*}|=4,|W_{46}^{*}|=3,|W_{55}^{*}|=2,|W_{56}^{*}|=2,|W_{57}^{*}|=2,|W_{58}^{*}|=1,|W_{59}^{*}|=1,|W_{66}^{*}|=5,$$
$$|W_{67}^{*}|=6,|W_{69}^{*}|=1,|W_{78}^{*}|=1,|W_{89}^{*}|=1.$$

By a designation of *NM*-polynomial

$$NM(H;p,q)=\sum_{\alpha\le\beta}m_{\alpha\beta}^{*}(H)p^{\alpha}q^{\beta}.$$

$$NM(SI;p,q)=\sum_{3\le5}m_{35}^{*}p^{3}q^{5}+\sum_{3\le6}m_{36}^{*}p^{3}q^{6}+\sum_{4\le6}m_{46}^{*}p^{4}q^{6}+\sum_{5\le5}m_{55}^{*}p^{5}q^{5}+\sum_{5\le6}m_{56}^{*}p^{5}q^{6}+\sum_{5\le7}m_{57}^{*}p^{5}q^{7}+\sum_{5\le8}m_{58}^{*}p^{5}q^{8}$$
$$+\sum_{5\le9}m_{59}^{*}p^{5}q^{9}+\sum_{6\le6}m_{66}^{*}p^{6}q^{6}+\sum_{6\le7}m_{67}^{*}p^{6}q^{7}+\sum_{7\le8}m_{78}^{*}p^{7}q^{8}+\sum_{8\le9}m_{89}^{*}p^{8}q^{9}.$$

The spatial depiction of *NM*-polynomials for Sitagliptin is depicted in Fig. 5 below.

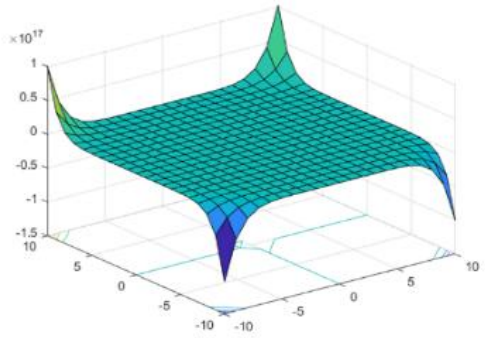

Fig. 5: Scheme of *NM*-polynomial for Sitagliptin.

In the following proposition, we derive several *TIs* of Sitagliptin.

Proposition 2. Let *SI* represent the graph of Sitagliptin. The following relationships are defined:

1. $NM_1(SI) = 352.$
2. $NM_2(SI) = 1038.$
3. $NmM_2(SI) = 0.99.$
4. $NREM_3(SI) = 12948.$
5. $NF(SI) = 2180.$
6. $NSDD(SI) = 50.17.$
7. $NIR(SI) = 5.35.$
8. $NH(SI) = 5.26.$
9. $NISI(SI) = 85.61.$
10. $NAZI(SI) = 1315.74.$
11. $NSCI(SI) = 8.82.$
12. $NOGA(SI) = 12.78.$
13. $NABC(GL) = 49.78.$

Similarly, we calculated the topological indices were calculated for 8 other diabetes drugs, and the results of these calculations are presented in Tables (3) and (4).

2 Topological indices and *QSPR*

Based on the aforementioned information, thirteen *TIs* were analyzed for ten diabetic drugs, with the results presented in Tables (3) and (4). The modeling of eight physical features, including *BP*, *EV*, *FP*, *MR*, *PSA*, *PO*, *MV*, and *IR*, was conducted for the drugs Sitagliptin, Vildagliptin, Empagliflozin, Gliclazide, Nataglinide, Tolazamide, Bromocriptine, Metformin, Alogliptin, and Miglitol, extracted from the ChemSpider database and presented in Table (2). Furthermore, the normality of these data was evaluated, and the correlations among them are detailed in Table (5).

Subsequently, a linear regression model was employed to evaluate and analyze the data.

The physical characteristics of pharmaceutical agents employed in the treatment of diabetes are detailed in Table (2).

Table 2. Physical features of diabetes drugs.

Drug name	*BP*	*EV*	*FP*	*MR*	*PSA*	*PO*	*MV*	*IR*
Sitagliptin	529.9	80.5	274.3	85.2	77	33.8	252.4	1.59
Vildagliptin	531.3	92.8	275.1	81.7	76	32.4	238.3	1.601
Empagliflozin	664.5	102.7	355.7	114.4	109	45.4	322.4	1.628
Gliclazide	-	-	-	84.4	87	33.5	239.2	1.624
Nateglinide	527.6	84.4	272.9	89.6	66	35.5	287.3	1.536

Tolazamide	484.5	79	246.8	82.5	90	32.7	237.9	1.61
Chlorpropamide	-	-	-	66.3	84	26.3	207.4	1.553
Metformin	172.5	40.9	58.1	33.4	89	13.2	100.8	1.576
Tolbutamide	-	-	-	70.8	84	28.1	228.3	1.532
Miglitol	453.7	82.3	284.3	48.5	104	19.2	142.1	1.598

The calculation results of section 2 are shown in Table (3),(4).

Table 3. The computed values of *TIs* for the pharmaceutical agents.

Drug name	NM_1	NM_2	NRM_3	NmM_2	*NF*	*NSDD*	*NH*
Sitagliptin	352.00	1038.00	.99	12948.00	2180.00	63.98	5.26
Vildagliptin	310.00	979.00	.79	12934.00	2022.00	50.61	4.22
Empagliflozin	388.00	1118.00	1.22	13522.00	2330.00	68.16	6.18
Gliclazide	274.00	787.00	.82	9446.00	1636.00	50.17	4.32
Nateglinide	252.00	668.00	.99	7440.00	1392.00	50.49	4.73
Tolazamide	232.00	620.00	.90	6081.00	1294.00	45.96	4.32
Chlorpropamide	72.00	162.00	.46	1283.00	1572.00	17.40	1.84
Metformin	154.00	437.00	.70	5474.00	948.00	29.32	5.65
Tolbutamide	177.00	485.00	.88	5318.00	1022.00	31.78	3.77
Miglitol	176.00	469.00	.82	5386.00	990.00	36.06	3.52

Table 4. The computed values of TIs for the pharmaceutical agents.

Drug name	*NISI*	*NAZI*	*NSCI*	*NIR*	*NOGA*	*NABC*
Sitagliptin	85.61	1315.74	8.82	5.35	12.48	49.78
Vildagliptin	76.03	1292.29	7.22	4.64	10.17	38.70
Empagliflozin	94.68	826.51	10.20	6.62	28.73	52.99
Gliclazide	67.10	942.75	7.09	4.32	9.94	37.32
Nateglinide	61.59	742.83	7.50	4.79	23.95	37.78
Tolazamide	56.77	761.91	6.86	4.37	21.77	34.64
Chlorpropamide	17.31	186.59	2.70	3.04	7.83	11.25
Metformin	36.62	546.30	4.38	2.75	13.59	22.08
Tolbutamide	44.78	33.53	5.77	3.83	12.28	27.55
Miglitol	42.78	576.27	5.42	3.58	16.75	26.94

3.1 Regression models

In this part, the evaluation is conducted using the *TIs* computed in Section 2. The linear regression framework is presented in the following manner:

$$P=B+A(TI) \tag{2}$$

Here, *P* denotes the features of the diabetes medication, *B* represents a constant, and *A* signifies the regression coefficient. This analysis was performed using *SPSS* software, integrating eight specific characteristics and thirteen *TIs* across a total of ten diabetes medications.

Utilizing equation (2), various linear regression models for *TIs* are presented as follows:

1. First Zagreb index [$NM_1(G)$]

BP=172.820+1.224 [$NM_1(G)$], EV=44.098+.144 [$NM_1(G)$], FP=84.812+.667 [$NM_1(G)$],

MR=24.830+.213 [$NM_1(G)$], PO=9.800+.085 [$NM_1(G)$], MV=88.513+.574 [$NM_1(G)$].

2. Second Zagreb index [$NM_2(G)$]

BP=206.942+.381 [$NM_2(G)$], EV=47.428+.046 [$NM_2(G)$], FP=102.394+.209 [$NM_2(G)$],

MR=31.943+.065 [$NM_2(G)$], PO=12.626+.026 [$NM_2(G)$], MV=108.878+.173 [$NM_2(G)$].

3. Redefined Third Zagreb index [$NReM_3(G)$]

BP=248.724+.027 [$NReM_3(G)$], EV=51.761+.003 [$NReM_3(G)$], FP=123.206+.015 [$NReM_3(G)$],

MR=40.103+.004 [$NReM_3(G)$], PO=15.867+.002[$NReM_3(G)$], MV=131.414+.012[$NReM_3(G)$].

4. Modified Second Zagreb index [$NmM_2(G)$]

BP=-12.833+570.881 [NmM2(G)], EV=24.108+65.098 [NmM2(G)], FP=-23.585+319.388 [NmM2(G)],

MR=-15.096+105.923 [NmM2(G)], PO=-6.062+42.092 [$NmM_2(G)$], MV=-35.718+304.934 [NmM2(G)].

5. Symmetric Division index [*NSDD(G)*]

BP=130.330+7.522 [NSDD(G)], EV=40.509+.856 [NSDD(G)], FP=63.698+4.054 [NSDD(G)],

MR=16.726+1.328 [NSDD(G)], PO=6.584+.528 [NSDD(G)], MV=64.940+3.619 [NSDD(G)],

6. Harmonic index [*NH(G)*]

BP=43.091+95.104 [NH(G)], EV=25.244+11.984 [NH(G)], FP=-34.966+62.483 [NH(G)],

MR=21.527+12.361 [NH(G)], PO=8.499+4.910 [NH(G)].

7. Inverse Sum index [*NISI(G)*]

BP=176.302+4.969 [NISI(G)], EV=44.514+.586 [NISI(G)], FP=87.253+2.698 [NISI(G)],

MR=24.595+.876 [NISI(G)], PO=9.707+.348 [NISI(G)], MV=87.488+2.368 [NISI(G)].

8. Sum Connectivity index [*NSCI(G)*]

BP=112.250+54.074 [NSCI(G)], EV=38.202+6.191 [NSCI(G)], FP=53.504+29.209 [NSCI(G)],

MR=8.597+10.170 [NSCI(G)], PO=3.352+4.042 [NSCI(G)], MV=39.735+28.180 [NSCI(G)].

9. Inverse Randić index [*NIR(G)*]

BP=74.329+90.104 [NIR(G)], MR=-4.334+18.483 [NIR(G)], PO=-1.783+7.344 [NIR(G)],

MV=5.958+50.740 [NIR(G)].

10. Neighborhood Ordinary Geometric Arithmetic index [*NOGA(G)*]

MR=40.960+2.205 [NOGA(G)], PO=16.234+.875 [NOGA(G)], MV=124.777+6.403 [NOGA(G)].

11. Atomic Bond Connectivity index [*NABC(G)*]

BP=152.521+9.289 [NABC(G)], EV=42.874+1.062 [NABC(G)], FP=74.294+5.045 [NABC(G)],

MR=18.311+1.692 [NABC(G)], PO=7.211+.672 [NABC(G)], MV=67.878+4.652 [NABC(G)].

Table 5. The computed values of correlation coefficients of physical features for the pharmaceutical agents.

TI	*DE*	*BP*	*EV*	*FP*	*MR*	*PSA*	*PO*	*ST*	*MV*	*IR*
NM_1	.313	.902	.832	.805	.914	.030	.914	.034	.864	.450
NM_2	.349	.882	.831	.793	.873	.032	.873	.016	.817	.476
NmM_2	.047	**.920**	.821	.844	.938	.057	.938	.210	**.945**	.115
NRM_3	.391	.848	.819	.775	.809	.036	.809	.078	.751	.474
NF	.377	.431	.356	.282	.578	.022	.578	.047	.490	.530
NSDD	.288	.898	.800	.794	.930	.062	.930	.104	.888	.415
NH	.436	.887	**.875**	**.955**	.667	.329	.667	.386	.625	.389
NISI	.297	.900	.830	.801	.919	.039	.920	.048	.871	.439
NAZI	.449	.688	.657	.614	.566	.247	.566	.116	.500	.543
NSCI	.194	.913	.818	.808	**.969**	.030	**.969**	.151	.941	.334
NIR	.121	.791	.683	.649	.929	.012	.929	.227	.894	.321
NOGA	.224	.681	.608	.632	.674	.228	.673	.079	.686	.032
NABC	.280	.904	.808	.804	.938	.054	.938	.129	.904	.370

Bold numbers indicate the strongest correlations.

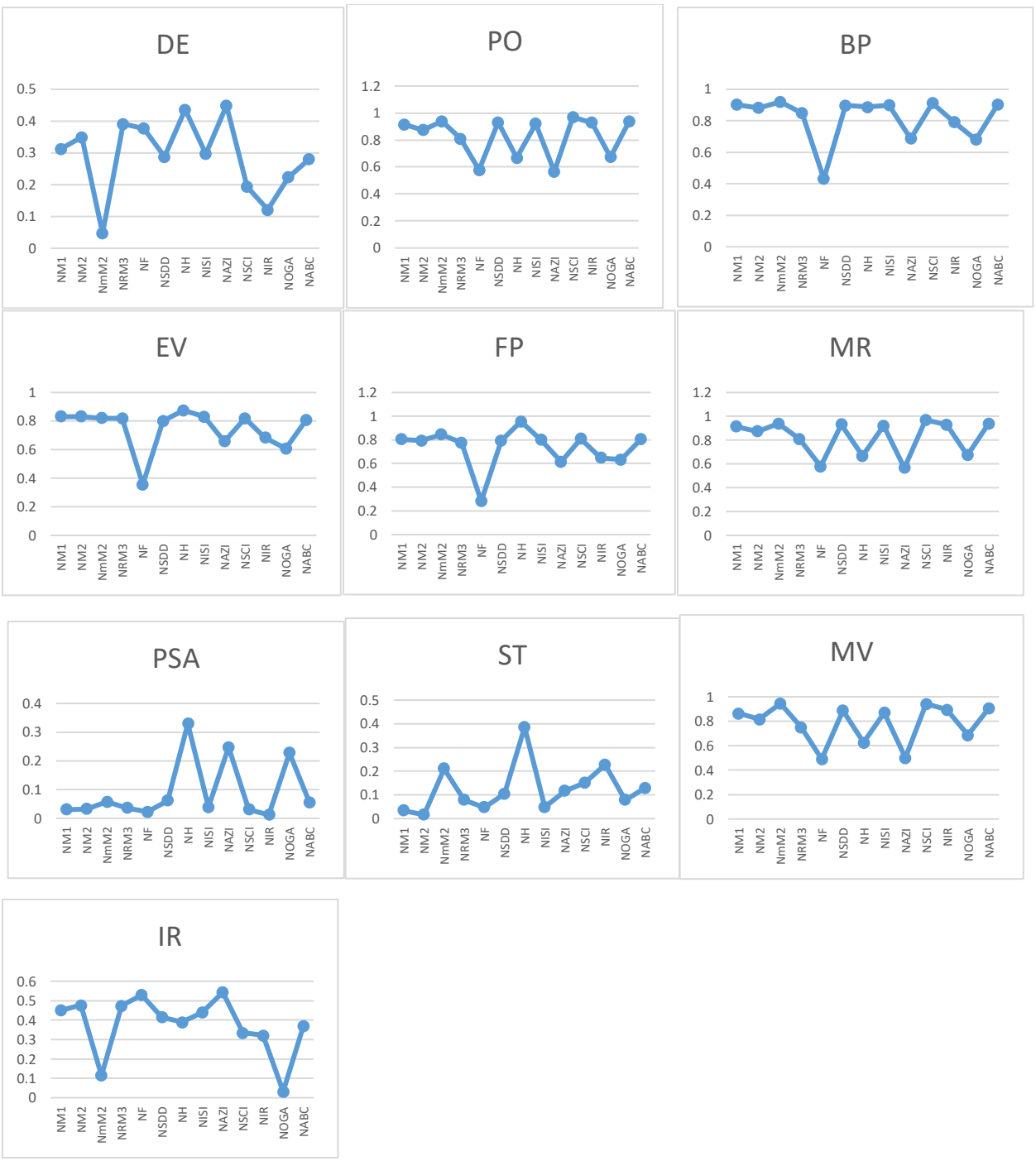

Fig. 6. Correlation coefficients on Physical features.

Table 6. Calculation of statistical metrics for the linear *QSPR* about *NM1*.

Physical features	*N*	*A*	*b*	*R*	R^2	*SE*	*F*	*P*	Indicant
BP	10	1.224	172.820	.902	.814	71.323	21.872	.005	significant
EV	10	.144	44.098	.832	.692	11.724	11.246	.020	significant
FP	10	.667	84.812	.805	.649	59.786	9.237	.029	significant
MR	10	.213	24.830	**.914**	**.836**	9.690	40.776	.000	significant
PO	10	.085	9.800	**.914**	**.836**	3.848	40.840	.000	significant
MV	10	.574	88.513	.864	.747	34.358	23.580	.001	significant
Bold numbers indicate the strongest correlations.									

Table 7. Calculation of statistical metrics for the linear *QSPR* about NM_2.

Physical features	*N*	*A*	*b*	*R*	R^2	*SE*	*F*	*P*	Indicant
BP	10	.381	206.942	.882	.778	77.970	17.485	.009	significant
EV	10	.046	47.428	.831	.690	11.766	11.130	.021	significant
FP	10	.209	102.394	.793	.628	61.510	8.450	.034	significant
MR	10	.065	31.943	.873	.762	11.677	25.593	.001	significant
PO	10	.026	12.626	**.873**	**.762**	4.637	25.643	.001	significant
MV	10	.173	108.878	.817	.667	39.403	16.011	.004	significant

Table 8. Calculation of statistical metrics for the linear *QSPR* about $NRzM_3$.

Physical features	*N*	*A*	*b*	*R*	R^2	*SE*	*F*	*P*	Indicant
BP	10	570.881	-12.833	.920	.847	64.616	27.739	.003	significant
EV	10	65.098	24.108	.821	.674	12.057	10.359	.024	significant
FP	10	319.388	-23.585	.844	.712	54.105	12.384	.017	significant
MR	10	105.923	-15.096	.938	.879	8.311	58.313	.000	significant
PO	10	42.092	-6.062	.938	.879	3.303	58.307	.000	significant
MV	10	304.934	-35.718	**.946**	**.895**	22.069	68.542	.000	significant

Table 9. Calculation of statistical metrics for the linear *QSPR* about NmM_2.

Physical features	*N*	*A*	*b*	*R*	R^2	*SE*	*F*	*P*	Indicant
BP	10	.027	248.724	**.848**	**.719**	87.677	12.782	.016	significant
EV	10	.003	51.761	.819	.670	12.138	10.156	.024	significant
FP	10	.015	123.206	.775	.600	63.797	7.503	.041	significant
MR	10	.004	40.103	.809	.654	14.067	15.147	.005	significant
PO	10	.002	15.867	.809	.655	5.586	15.179	.005	significant
MV	10	.012	131.414	.751	.564	45.092	10.334	.012	significant

Table 10. Calculation of statistical metrics for the linear *QSPR* about *NF*.

Physical features	*N*	*A*	*b*	*R*	R^2	*SE*	*F*	*P*	Indicant
BP	10	7.522	130.330	.898	.807	72.616	20.923	.005	significant
EV	10	.856	40.509	.800	.640	12.679	8.891	.031	significant
FP	10	4.054	63.698	.794	.630	61.387	8.504	.033	significant
MR	10	1.328	16.726	**.930**	**.864**	8.818	50.904	.000	significant
PO	10	.528	6.584	**.930**	**.864**	3.506	50.853	.000	significant
MV	10	3.619	64.940	.888	.789	31.380	29.857	.001	significant

Table 11. Calculation of statistical metrics for the linear *QSPR* about *NSDD*.

Physical features	*N*	*A*	*b*	*R*	R^2	*SE*	*F*	*P*	Indicant
BP	10	95.104	43.091	.887	.787	76.333	18.459	.008	significant
EV	10	11.984	25.244	.875	.765	10.246	16.268	.010	significant
FP	10	62.483	-34.966	**.955**	**.912**	29.867	52.048	.001	significant
MR	10	12.361	21.527	.667	.445	17.824	6.419	.035	significant
PO	10	4.910	8.499	.667	.445	7.085	6.410	.035	significant

Table 12. Calculation of statistical metrics for the linear *QSPR* about *NH*.

Physical features	*N*	*A*	*b*	*R*	R^2	*SE*	*F*	*P*	Indicant
BP	10	4.969	176.302	.900	.811	71.963	21.396	.006	significant
EV	10	.586	44.514	.830	.689	11.782	11.085	.021	significant
FP	10	2.698	87.253	.801	.642	60.372	8.962	.030	significant
MR	10	.876	24.595	.919	.845	9.409	43.741	.000	significant
PO	10	.348	9.707	**.920**	**.846**	3.736	43.829	.000	significant
MV	10	2.368	87.488	.871	.759	33.486	25.246	.001	significant

Table 13. Calculation of statistical metrics for the linear *QSPR* pertaining to *NISI*.

Physical features	*N*	*A*	*b*	*R*	R^2	*SE*	*F*	*P*	Indicant
BP	10	54.074	112.250	.913	.834	67.421	25.072	.004	significant
EV	10	6.191	38.202	.818	.669	12.157	10.108	.025	significant
FP	10	29.209	53.504	.808	.653	59.389	9.4288	.028	significant
MR	10	10.170	8.597	**.969**	**.940**	5.881	124.429	.000	significant
PO	10	4.042	3.352	**.969**	**.940**	2.336	124.555	.000	significant
MV	10	28.180	39.735	.941	.886	23.0105	62.406	.000	significant

Table 14. Calculation of statistical metrics for the linear *QSPR* about *NAZI*.

Physical features	*N*	*A*	*b*	*R*	R^2	*SE*	*F*	*P*	Indicant
BP	10	90.104	74.329	.791	.625	101.187	8.351	.034	significant
MR	10	18.483	-4.334	**.929**	**.863**	8.867	50.265	.000	significant
PO	10	7.344	-1.783	**.929**	**.863**	3.526	50.195	.000	significant
MV	10	50.740	5.958	.894	.799	30.617	31.769	.000	significant

Table 15. Calculation of statistical metrics for the linear *QSPR* about *NSCI*.

Physical features	*N*	*A*	*b*	*R*	R^2	*SE*	*F*	*P*	Indicant
MR	10	2.205	40.960	.674	.454	17.68	6.655	.033	significant
PO	10	.875	16.234	.673	.453	7.034	6.618	.033	significant
MV	10	6.403	124.777	**.686**	**.471**	49.668	7.112	.029	significant

Table 16. Calculation of statistical metrics for the linear *QSPR* about *NIR*.

Physical features	*N*	*A*	*b*	*R*	R^2	*SE*	*F*	*P*	Indicant
BP	10	9.289	152.521	.904	.817	70.787	22.280	.005	significant
EV	10	1.062	42.874	.808	.653	12.444	9.419	.028	significant
FP	10	5.045	74.294	.804	.647	59.932	9.168	.029	significant
MR	10	1.692	18.311	**.938**	.880	8.274	58.911	.000	significant
PO	10	.672	7.211	**.938**	**.881**	3.286	58.985	.000	significant
MV	10	4.652	67.878	.904	.818	29.139	35.904	.000	significant

4 CONCLUSION

This study successfully demonstrates the efficacy of the novel *NM*-polynomial approach in computing neighborhood degree sum-based topological indices for *QSPR* analysis of anti-diabetic drugs. Our comprehensive investigation of ten prominent anti-diabetic medications reveals strong, statistically significant correlations between the computed topological indices and key physicochemical properties.

The exceptional predictive performance of specific indices is particularly noteworthy. The Neighborhood Modified Second Zagreb index (NmM_2) emerged as an outstanding descriptor for Boiling Point and Molar Volume (r = 0.920 and r = 0.945, respectively), while the Neighborhood Sum Connectivity index (*NSCI*) demonstrated remarkable predictive power for Molar Refractivity and Polarizability (r = 0.969 for both). Additionally, the Neighborhood Harmonic index (*NH*) showed strong correlation with Flash Point (r = 0.955).

The developed linear regression models, characterized by high correlation coefficients ($r > 0.8$ in most cases), significant p-values ($p < 0.05$), and substantial R^2 values, validate the reliability of our approach. The *NM*-polynomial method proved to be an efficient computational framework for simultaneous derivation of multiple topological indices, offering significant advantages over traditional calculation methods.

These findings have substantial implications for pharmaceutical research, providing a robust computational tool for predicting physicochemical properties of potential anti-diabetic compounds prior to synthesis. This approach can significantly accelerate drug discovery processes and reduce development costs.

Future research directions include extending this methodology to larger datasets of drug molecules, exploring non-linear machine learning models for enhanced predictive accuracy, and investigating *3D* topological descriptors to provide more comprehensive structure-property relationship insights.

Authors' declaration

•Conflicts of Interest: None.

•We hereby confirm that all the Figures and Tables in the manuscript are ours.

•No animal studies are present in the manuscript.

• No human studies are present in the manuscript.

Acknowledgments

The authors are very grateful to the editor and the anonymous referee(s) for their comments and suggestions which led to the present improved version of the manuscript.

Data Availability Statement: All relevant data are within the article.

Use of *AI* tools declaration: The authors declare they have not used Artificial Intelligence (*AI*) tools in the creation of this article.

REFERENCES

1- Eller-Vainicher, C., Cairoli, E., Grassi, G., Grassi, F., Catalano, A., Merlotti, D., Gennari, L. (2020). Pathophysiology and management of type 2 diabetes mellitus bone fragility. *Journal of Diabetes Research*, *2020*(1), 7608964.
2- American Diabetes Association. (2011). Standards of medical care in diabetes—2011. *Diabetes care*, *34*(Supplement_1), S11-S61.
3- Gross, J. L., Yellen, J., Anderson, M. (2018). *Graph theory and its applications*. Chapman and Hall/CRC.
4- Kumar, K. A., Basavarajappa, N. S., Shanmukha, M. C. (2020). QSPR analysis of Alkanes with certain degree based topological indices. *Malaya Journal of Mathematik*, *8*(1), 314-30.
5- Gutman, I., Trinajstić, N. (1972). Graph theory and molecular orbitals. Total φ-electron energy of alternant hydrocarbons. *Chemical physics letters*, *17*(4), 535-538.
6- Ramezani Tousi, J., Ghods, M. (2024). Computational Analysis of the Molecular Graph and the Line Graph of Glass by Studying Their *M*-Polynomial and Topological indices. *Discontinuity, Nonlinearity, and Complexity*, 13(02), 361-371.
7- Yang, H., Baig, A. Q., Khalid, W., Farahani, M. R., Zhang, X. (2019). M-Polynomial and Topological Indices of Benzene Ring Embedded in P-Type Surface Network. *Journal of Chemistry*, *2019*(1), 7297253.
8- Furtula, B., Gutman, I. (2015). A forgotten topological index. *Journal of mathematical chemistry*, *53*(4), 1184-1190.
9- Sedlar, J., Stevanović, D., Vasilyev, A. (2015). On the inverse sum indeg index. *Discrete Applied Mathematics*, *184*, 202-212.
10- Shi, X., Cai, R., Ramezani Tousi, J., Talebi, A. A. (2024). Quantitative Structure–Property Relationship Analysis in Molecular Graphs of Some Anticancer Drugs with Temperature Indices Approach. *Mathematics*, 12(13), 1953.

11- Shi, X., Kosari, S., Ghods, M., Kheirkhahan, N. Innovative approaches in *QSPR* modelling using topological indices for the development of cancer treatments. Plos one, 2025, 20: 1-19.
12- Javame, S., Ramezani Tousi, J., Ghods, M. (2025).Investigating new Revan indices on *V*-Phenylenic nanotube and nanotori with *M*-polynomial approach. *Journal of Interdisciplinary Mathematics*, 28(2), 499–520.
13- Ramezani Tousi, J., Ghods, M. (2024). Some polynomials and degree-based topological indices of molecular graph and line graph of Titanium dioxide nanotubes. *Journal of Information and Optimization Sciences*, *1*(2), 15-25.
14- Al-Dayel, I., Khan, M. A., Hanif, M. F., Siddiqui, M. K., Hanif, S., Gegbe, B. (2025). A graph-based computational approach for modeling physicochemical properties in drug design. *Scientific Reports*, *15*(1), 21170.
15- Ramezani Tousi, J., Ghods, M. (2024). Investigating Banhatti indices on the molecular graph and the line graph of Glass with *M*-polynomial approach. *Proyecciones (Antofagasta)*, 43(1), 225-245.
16- Aqib, M., Ali Malik, M., Usman Afzal, H., Fatima, T., Ali, Y. (2023). On topological indices of some chemical graphs. *Molecular Physics*, e2276386.
17- Ali, H., Binyamin, M. A., Shafiq, M. K., Gao, W. (2019). On the degree-based topological indices of some derived networks. *Mathematics*, *7*(7), 612.
18- Parveen, S., Hassan Awan, N. U., Mohammed, M., Farooq, F. B., Iqbal, N. (2022). Topological indices of novel drugs used in diabetes treatment and their *QSPR* modeling. *Journal of Mathematics*, 2022(1), 5209329.
19- Gambhire, S. N., Ghods, M., Rostami, Z. (2025). Sombor Index in Neutrosophic Graphs. *Neutrosophic Sets and Systems*, 82, 2025, 431.
20- Hasani, M., Ghods, M., Mondal, S., Siddiqui, M. K., Cheema, I. Z. (2025). Modeling *QSPR* for pyelonephritis drugs: a topological indices approach using MATLAB. *The Journal of Supercomputing*, 81(3), 479.
21- Sadati, S., Talebi, A. A. (2023). A Description of Connectivity Indices in a Cubic Fuzzy Graph With an Application. *Journal of Multiple-Valued Logic and Soft Computing*, 40.
22- Guan, H., Sadati, S. H., Talebi, A. A., Shafi, J., Khan, A. (2024). A connectivity index based on adjacent vertices in cubic fuzzy graph with an application. *Journal of Intelligent and Fuzzy systems*, 46(2024), 11025-11040.